

Spinodal decomposition in polarised Fermi superfluids

A. Lamacraft* and F. M. Marchetti†

Rudolf Peierls Centre for Theoretical Physics, 1 Keble Road, Oxford OX1 3NP, UK

(Dated: January 28, 2007)

We discuss the dynamics of phase separation through the process of spinodal decomposition in a Fermi superfluid with population imbalance. We discuss this instability first in terms of a phenomenological Landau theory. Working within the mean-field description at zero temperature, we then find the spinodal region in the phase diagram of polarisation versus interaction strength, and the spectrum of unstable modes in this region. After a quench, the spinodal decomposition starts from the Sarma state, which is a minimum of the free energy with respect to the order parameter *at fixed density and polarisation* and a maximum at fixed chemical potentials. The possibility of observing non-trivial domain structures in current experiments with trapped atomic gases is discussed.

PACS numbers: 03.75.Kk, 03.75.Ss, 64.75.+g

The ordering of matter into different phases is a central preoccupation of many areas of physics, from condensed matter to cosmology. Hand in hand with the *existence* of different phases goes the question of the dynamical processes responsible for their formation, which may be equally important in determining what is observed in a given situation. Recent experimental advances in the creation of degenerate atomic gases have begun to realize the prospect of a rich variety of new phases in atomic matter, involving the hyperfine degrees of freedom, mixtures of different species, or spatial order on optical lattices. With each new phase comes the dynamical issue of how that phase will appear under laboratory conditions. One advantage offered by atomic systems is that the characteristic timescale $\hbar/k_B T$ at nanokelvin temperatures is in the convenient millisecond range.

The possibility of tuning interparticle interactions in a controlled manner has proven to be of particular significance lately. Magnetically tuned Feshbach resonances have permitted the experimental investigation of the crossover from a Bose-Einstein condensate (BEC) of diatomic molecules to the Bardeen-Cooper-Schrieffer (BCS) limit of weakly-bound Cooper pairs of fermionic atoms^{1,2,3,4,5,6}.

It appears that when the numbers of atoms of the two species undergoing pairing are equal, the system forms a condensate with smoothly varying properties at low temperatures. With unequal numbers (we will call such a system ‘polarised’) there is the possibility of phase separation into a superfluid of low polarisation (favoured by pairing) and a normal fluid of higher polarisation^{7,8,9,10,11,12,13}.

With the occurrence of phase separation in these systems now established, it is crucial to examine the dynamics of this process, and that is the purpose of this Letter. Working within a mean-field approximation, we find that the dome of phase separation at temperatures below the tricritical point^{14,15} contains a *spinodal* region where phase separation proceeds via a linear instability. In many recent papers this region is incorrectly identified with the phase coexistence region^{16,17,18,19} (see Fig. 1).

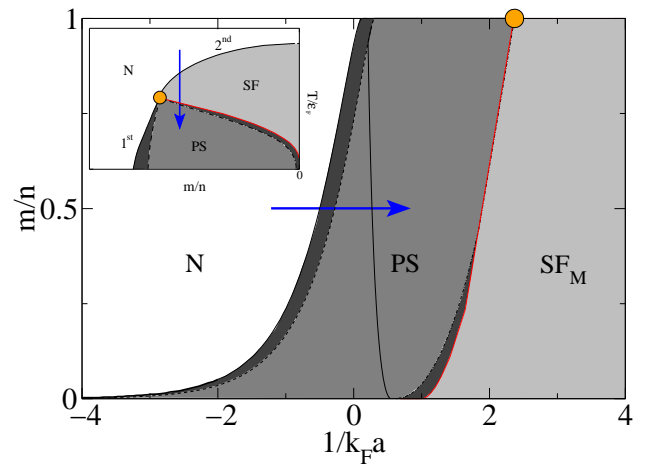


FIG. 1: (Colour online) Zero temperature mean-field phase diagram for magnetisation m/n versus interaction strength $1/k_F a$. The phase separated region (PS) can be decomposed into two regions — the spinodal or unstable region and the metastable region (darker shade) — divided by the spinodal normal (sp-N) line (dashed) and the spinodal superfluid (sp-SF) line (dot-dashed). In addition, the PS spinodal phase is divided in half by the line where the superfluid density Q is zero (thin solid). The tricritical point (orange circle) is at $m/n = 1$ and $1/k_F a \simeq 2.37$. Inset: schematic finite temperature phase diagram of T_c/ε_F versus m/n for a fixed interaction strength $1/k_F a$. Arrows indicate possible quenches into the spinodal region.

We discuss the dynamics initiated by a quench into the spinodal region by finding the unstable density modes associated with the endpoint of the quench. The modes with the fastest growth rate give the characteristic size of the resulting domains of superfluid and normal fluid. Though our description of these processes will not be quantitatively correct in the crossover region where the system is strongly interacting, we emphasise that this behaviour is a generic feature of systems possessing this type of phase diagram. In particular, our system shares many similarities with the problem of ^3He - ^4He mixtures

(see e.g.^{20,21}). We will confine ourselves to the early stages of spinodal decomposition characterized by the exponential growth of unstable modes. The emergence of a coarsening regime at later times, where domains scale with the time since the quench²², is a fascinating possibility that we will leave for future work.

The rest of this paper is organized as follows. In the next section we introduce a simple phenomenological model for the polarized system. We use this model to show how, with a simplifying assumption, mean-field calculations within the grand canonical ensemble may be applied to the early stages of spinodal decomposition. By adding dynamical assumptions, the equation satisfied by the sound velocity can be inferred. In section II we provide a microscopic mean-field calculation of the spectra of unstable modes, which are discussed in some detail in section III before we conclude.

I. PHENOMENOLOGICAL MODEL

We begin by discussing the phase diagram in phenomenological terms starting from a model free energy depending on the superfluid order parameter Δ and the density difference $m = n_{\uparrow} - n_{\downarrow}$, following a similar approach to the ³He-⁴He system²³

$$f_m(\Delta, m) \equiv \frac{r}{2}|\Delta|^2 + u|\Delta|^4 + v|\Delta|^6 + \frac{1}{2}\chi_n^{-1}m^2 + \gamma m|\Delta|^2. \quad (1)$$

The potential for Δ is the simplest one that can describe a first order transition. We are interested in $r < 0$ so that for $m = 0$ there is always superfluid order $\Delta \neq 0$. Further, the coupling to m has the obvious physical meaning that larger polarisations discourage pairing. We ignore for the moment additional couplings to the total density $n = n_{\uparrow} + n_{\downarrow}$ ³⁰.

Minimising (1) on the order parameter, gives the potential

$$F(m) \equiv \min_{\Delta} f_m(\Delta, m). \quad (2)$$

Where the transition is first order, the phase coexistence region ($m_{\text{cr-SF}}, m_{\text{cr-N}}$) is obtained by the usual tangent construction²⁴. Inside the coexistence region one identifies a spinodal region ($m_{\text{sp-N}}, m_{\text{sp-SF}}$), where the susceptibility $\partial_m^2 F(m) < 0$, and phase separation proceeds via the growth of unstable modes. In general this represents an extremely difficult dynamical problem. We will make the simplifying assumption that following a quench into the spinodal region, the order parameter relaxes rapidly to its minimum at fixed m , while $m(\mathbf{r})$, being a conserved quantity, begins to develop inhomogeneities on a much longer timescale. For the case of trapped gases, we will review the validity of this approach *a posteriori*.

Often it is convenient, particularly in many body calculations, to work instead with the grand canonical po-

tential $f_h(\Delta, h)$, obtained from f_m in the usual way

$$f_h(\Delta, h) \equiv \min_m [f_m(\Delta, m) - hm] = \frac{1}{2}\tilde{r}|\Delta|^2 + \tilde{u}|\Delta|^4 + v|\Delta|^6 - \frac{1}{2}\chi_n h^2, \quad (3)$$

where $\tilde{r} = r + 2\gamma h\chi_n$ and $\tilde{u} = u - \frac{1}{2}\chi_n\gamma^2 < 0$. If we assume $u > 0$, then for small γ a second order transition occurs when \tilde{r} changes sign. Increasing γ causes the transition to become first order as \tilde{u} becomes negative. Minimising $f_h(\Delta, h)$ on Δ gives the thermodynamic free energy $\Omega(h) \equiv \min_{\Delta} f_h(\Delta, h)$. At some critical $h = h_{\text{cr}}$ there is a discontinuity in the derivative (see Fig. 2). In a uniform phase $m = -\partial_h \Omega$ so the boundaries of the phase coexistence region are $m_{\text{cr-N,cr-SF}} = -\partial_h \Omega|_{h_{\text{cr}}^{\pm}}$. The two phases correspond to the two minima of $f_h(\Delta, h)$: one at $\Delta = 0$, the normal phase, and the superfluid phase at finite Δ . One can continue past h_{cr} on the metastable minimum, rather than the true minimum. Such states are linearly stable, with a positive susceptibility $-\partial_h^2 \Omega (= [\partial_m^2 F(m)]^{-1})$, since one may easily see that

$$\frac{\partial^2 \Omega}{\partial h^2} = \frac{\partial^2 f_h}{\partial h^2} - \left(\frac{\partial^2 f_h}{\partial \Delta^2} \right)^{-1} \left(\frac{\partial m}{\partial \Delta} \right)^2, \quad (4)$$

and the first term on the right hand side is $-\chi_n < 0$ — the normal state susceptibility is assumed positive. Since the curvature of $\Omega(h)$ remains negative, m takes values inside the coexistence region but the system remains uniform. This is of course not the equilibrium state of the system, but the other phase must nucleate in order for phase separation to occur.

This situation changes when the metastable minima merge with the maximum, for h corresponding respectively to $m_{\text{sp-N}}$ and $m_{\text{sp-SF}}$ for the metastable superfluid and normal phases. As already discussed, inside the spinodal region we seek the *constrained minimum* of $f_m(\Delta, m)$ with respect to Δ at fixed m , and the spectrum of unstable modes about this point. How should this programme be implemented for a many-body calculation that provides instead the grand canonical potential $f_h(\Delta, h)$? Fortunately, one may easily show that the stationary points of $f_m(\Delta, m)$ with respect to Δ coincide with those of $f_h(\Delta, h)$ at corresponding values of h and m . This is because $f_m(\Delta, m)$ may be written as

$$f_m(\Delta, m) = f_h(\Delta, h^*(\Delta, m)) + h^*(\Delta, m)m,$$

where $h^*(\Delta, m)$ is the value of h that maximises $f_h(\Delta, h) + hm$. Thus $m = -\partial_h \Omega|_{h=h^*}$. We can then easily see that the conditions, $\partial_{\Delta} f_m(\Delta, m) = 0$ and $\partial_{\Delta} f_h(\Delta, h) = 0$ are equivalent when $h = h^*(\Delta, m)$.

In the spinodal region the unstable constrained minimum corresponds to a *maximum* of f_h , as may be seen from Eq. (4): $\partial^2 \Omega / \partial h^2 > 0$ requires $\partial^2 f_h / \partial \Delta^2 < 0$. In the context of the mean-field theory for the paired fermion system, this corresponds to the solution of the self-consistent equation in a magnetic field discovered by Sarma²⁵.

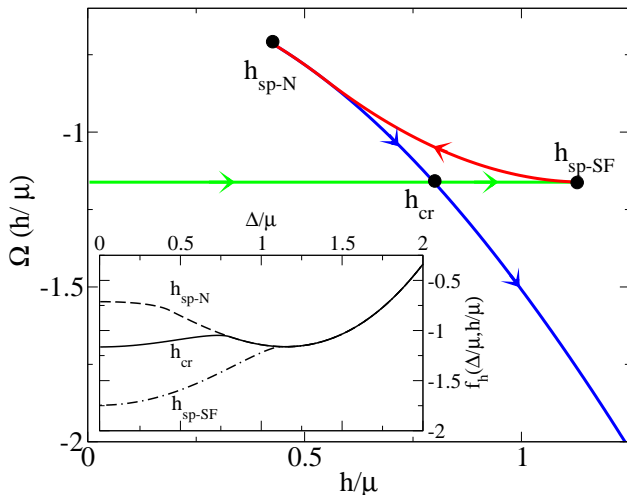


FIG. 2: (Colour online) Mean-field free energy $\Omega(h/\mu)$ for the Hamiltonian (7) versus h/μ at unitarity $1/k_F a = 0$ ($\mu > 0$) obtained evaluating the free energy density $f_h(\Delta/\mu, h/\mu)$ respectively at the local minimum for $\Delta/\mu \simeq 1.15$ (green), at $\Delta = 0$ (blue) and at the local maxima (red), i.e. the Sarma state. The value of h/μ corresponding to the spinodal-normal point (sp-N), the spinodal-superfluid point (sp-SF) and the critical value for phase separation (cr) are indicated. At unitarity, the corresponding values of the magnetisation are respectively $m_{\text{cr-SF}}/n = m_{\text{sp-SF}}/n = 0$, $m_{\text{sp-N}}/n \simeq 0.73$ and $m_{\text{cr-N}}/n \simeq 0.93$ (see Fig. 1). Inset: Plots of the free energy density $f_h(\Delta/\mu, h/\mu)$ for the values of h corresponding to $h_{\text{sp-N}}$, $h_{\text{sp-SF}}$ and h_{cr} . Note that the thermodynamic free energy corresponding to the Sarma state has a positive curvature indicating instability. The cusp structure shrinks to a point at the tricritical point.

These results are readily adapted to the presence of a trap potential $V(\mathbf{r})$ using the following simple approximation: At each point in space we find the *constrained minimum* of the order parameter for fixed local magnetisation $m(\mathbf{r})/n(\mathbf{r})$ corresponding to the density profiles before the quench. Spinodal decomposition therefore occurs where the local magnetisation lies in the spinodal region of the homogeneous phase diagram. Moving out from the centre of the trap corresponds to a vertical trajectory in Fig. 1 which will be displaced horizontally by a quench in $1/k_F a$.

To make contact with the microscopic analysis of the next section, let us add appropriate dynamics to the above model. Expanding $\Delta_0 + \delta\Delta$ around some value we write a phenomenological quadratic Lagrangian for the longitudinal (amplitude) and transverse (phase) modes

$$\mathcal{L} = B\delta\Delta_L\delta\dot{\Delta}_T + \frac{R}{2}(\delta\dot{\Delta}_T)^2 - \frac{Q}{2}(\nabla\delta\Delta_T)^2 - \frac{A}{2}(\delta\Delta_L)^2 - 2\gamma m\Delta_0\delta\Delta_L. \quad (5)$$

Eq. (5) includes all terms up to second order in the derivatives except for a $(\delta\dot{\Delta}_T)^2$ term that will not change the sound velocity. $\delta\Delta_L$ is coupled to the density difference

m as specified in the model Eq. (1). m is written in terms of the distribution function of the majority quasiparticle distribution function (at zero temperature there are no minority quasiparticles)

$$m(\mathbf{r}) = \sum_{\mathbf{p}} n_{\uparrow}(\mathbf{p}, \mathbf{r}),$$

which obeys the Boltzmann equation

$$[\partial_t + \mathbf{v}_F \cdot \nabla_{\mathbf{r}} - 2\gamma\Delta_0\nabla_{\mathbf{r}}\delta\Delta_L \cdot \nabla_{\mathbf{p}}] n_{\uparrow}(\mathbf{p}, \mathbf{r}, t) = 0.$$

where $\mathbf{v}_F = v_F\hat{\mathbf{p}}$ is the Fermi velocity. The linearized solution is expressed as

$$n_{\uparrow}(\mathbf{p}, \mathbf{q}, \omega) = \frac{\mathbf{q} \cdot \mathbf{v}_F}{\omega - \mathbf{v}_F \cdot \mathbf{q}} 2\gamma\Delta_0\delta\Delta_L(\mathbf{q}, \omega)\delta(\epsilon_{\mathbf{p}} - \mu)$$

$$m(\mathbf{q}, \omega) = 2\gamma\Delta_0\nu(\mu)L(\omega/|\mathbf{q}|)\delta\Delta_L(\mathbf{q}, \omega)$$

where $L(x) = \frac{x}{2} \log \frac{x+1}{x-1} - 1$ is the Lindhard function, and $\nu(\mu)$ the Fermi surface density of states. The dispersion relation of the linearized modes is then given by a solution of

$$\begin{vmatrix} A & iB\omega & 2\gamma\Delta_0 \\ -iB\omega & Qq^2 - R\omega^2 & 0 \\ 2\gamma\Delta_0\nu(\mu)L(\omega/|\mathbf{q}|) & 0 & -1 \end{vmatrix} = 0,$$

or

$$(A + 4\gamma^2\Delta_0^2\nu L(c_s))(Q - Rc_s^2) - B^2c_s^2 = 0. \quad (6)$$

We will see that an equation of the same form emerges from the microscopic analysis of the next section, where the solutions will be further analyzed.

II. MICROSCOPIC CALCULATION

We turn now to the analysis of the microscopic problem described by the Hamiltonian

$$\hat{H} - \sum_{\sigma=\uparrow,\downarrow} \mu_{\sigma} \hat{n}_{\sigma} = \sum_{\mathbf{k}\sigma} (\epsilon_{\mathbf{k}} - \mu_{\sigma}) c_{\mathbf{k}\sigma}^{\dagger} c_{\mathbf{k}\sigma} + \frac{g}{V} \sum_{\mathbf{k}, \mathbf{k}', \mathbf{q}} c_{\mathbf{k}+\mathbf{q}/2\uparrow}^{\dagger} c_{-\mathbf{k}+\mathbf{q}/2\downarrow}^{\dagger} c_{-\mathbf{k}'+\mathbf{q}/2\downarrow} c_{\mathbf{k}'+\mathbf{q}/2\uparrow}, \quad (7)$$

where $\epsilon_{\mathbf{k}} = k^2/2m$ (we set $\hbar = 1$) and where the scattering length is introduced in the usual way:

$$\frac{1}{g} = \frac{m}{4\pi a} - \frac{1}{V} \sum_{\mathbf{k}} \frac{1}{2\epsilon_{\mathbf{k}}}. \quad (8)$$

The condition $\partial^2 f_h / \partial \Delta^2 = 0$, corresponding to a divergent susceptibility, was used to obtain the spinodal lines in Fig. 1. As explained before, the unstable modes are to be found from the matrix response function (dynamical susceptibility):

$$\hat{\chi}(\mathbf{r} - \mathbf{r}', t - t')$$

$$= -i \begin{pmatrix} \langle [n(\mathbf{r}, t), n(\mathbf{r}', t')] \rangle & \langle [n(\mathbf{r}, t), m(\mathbf{r}', t')] \rangle \\ \langle [m(\mathbf{r}, t), n(\mathbf{r}', t')] \rangle & \langle [m(\mathbf{r}, t), m(\mathbf{r}', t')] \rangle \end{pmatrix}. \quad (9)$$

Finding the spectrum of collective modes requires us to solve the equation

$$\det \hat{\chi}^{-1}(\mathbf{q}, \varepsilon(\mathbf{q})) = 0, \quad (10)$$

which defines the dispersion relation $\varepsilon(\mathbf{q})$. The unstable modes correspond to $\Im\varepsilon(\mathbf{q}) > 0$. In practice, the response matrix (9) can be found making use of a path integral formulation, by expanding the action

$$S[\Delta, \mu, h] = -\frac{1}{g} \int_0^\beta d\tau \int d\mathbf{r} |\Delta|^2 - \text{tr} \ln \hat{\mathcal{G}}^{-1} \quad (11)$$

$$\hat{\mathcal{G}}^{-1} = \begin{pmatrix} \partial_\tau - \frac{\nabla^2}{2m} - \mu - h & -\Delta \\ -\Delta^* & \partial_\tau + \frac{\nabla^2}{2m} + \mu - h \end{pmatrix},$$

up to second order in fluctuations of $\mu(\mathbf{r}, \tau) = \mu + \delta\mu(\mathbf{r}, \tau)$, $h(\mathbf{r}, \tau) = h + \delta h(\mathbf{r}, \tau)$ and $\Delta(\mathbf{r}, \tau) = \Delta + \delta\Delta^L(\mathbf{r}, \tau) + i\delta\Delta^T(\mathbf{r}, \tau)$ around their mean-field values. Here, we have introduced $\mu = (\mu_\uparrow + \mu_\downarrow)/2$ and $h = \mu_\uparrow - \mu_\downarrow$.

By completing the squares in $\delta\Delta^L$ and $\delta\Delta^T$, one can easily obtain:

$$\hat{\chi}(\mathbf{q}, i\omega_h) = \begin{pmatrix} \Pi_{\mu\mu} & \Pi_{h\mu} \\ \Pi_{\mu h} & \Pi_{hh} \end{pmatrix} - \begin{pmatrix} \Pi_{\mu\Delta^L} & \Pi_{\mu\Delta^T} \\ \Pi_{h\Delta^L} & \Pi_{h\Delta^T} \end{pmatrix} \hat{\mathcal{D}} \begin{pmatrix} \Pi_{\Delta^L\mu} & \Pi_{\Delta^L h} \\ \Pi_{\Delta^T\mu} & \Pi_{\Delta^T h} \end{pmatrix}, \quad (12)$$

where we have introduced the polarization operators

$$\Pi_{ab}(\mathbf{q}, i\omega_h) = \frac{1}{V\beta} \sum_{\mathbf{k}, i\epsilon_n} \text{tr} \tau_a \hat{G}_{\mathbf{q}+\mathbf{k}, i\epsilon_n + i\omega_h} \tau_b \hat{G}_{\mathbf{q}, i\epsilon_n}^{(0)},$$

with $\tau_\mu = \sigma_3$, $\tau_h = \mathbb{1}$, $\tau_{\Delta^L} = \sigma_1$, and $\tau_{\Delta^T} = \sigma_2$, and where the order parameter propagator is

$$\hat{\mathcal{D}}^{-1} = -\frac{2}{g} \mathbb{1} + \begin{pmatrix} \Pi_{\Delta^L\Delta^L} & \Pi_{\Delta^L\Delta^T} \\ \Pi_{\Delta^T\Delta^L} & \Pi_{\Delta^T\Delta^T} \end{pmatrix}. \quad (13)$$

We omit the explicit expressions for these quantities, as they are straightforward generalisations of the expressions found e.g. in Ref. 26 to the case $h \neq 0$. It is clear that Eq. (12) is the generalisation of Eq. (4) to the full matrix response and to nonzero \mathbf{q} and ε .

The mean-field approximation to the mode spectrum is the solution of Eq. (10), with the response matrix given by the expression (12). Here, μ and h are chosen so that n and m take the desired values, and inside the spinodal region, Δ is taken at the Sarma value corresponding to the maximum of $f_h(\Delta, h)$ — as discussed, the stationary points of $f_h(\Delta, h)$ coincide with those of $f_m(\Delta, m)$. Evidently, a sufficient condition for a solution of Eq. (10) is the occurrence of a pole at $\varepsilon(\mathbf{q})$ in the order parameter propagator, so we must solve $\det \hat{\mathcal{D}}^{-1}(\mathbf{q}, \varepsilon(\mathbf{q})) = 0$. In general, a numerical solution is called for. At the spinodal lines, however, a diverging susceptibility implies a vanishing sound velocity, which we can find by expanding in ε and \mathbf{q} :

$$\hat{\mathcal{D}}^{-1} \simeq \begin{pmatrix} A + P(\varepsilon/q) & iB\varepsilon \\ -iB\varepsilon & Qq^2 - R\varepsilon^2 \end{pmatrix}, \quad (14)$$

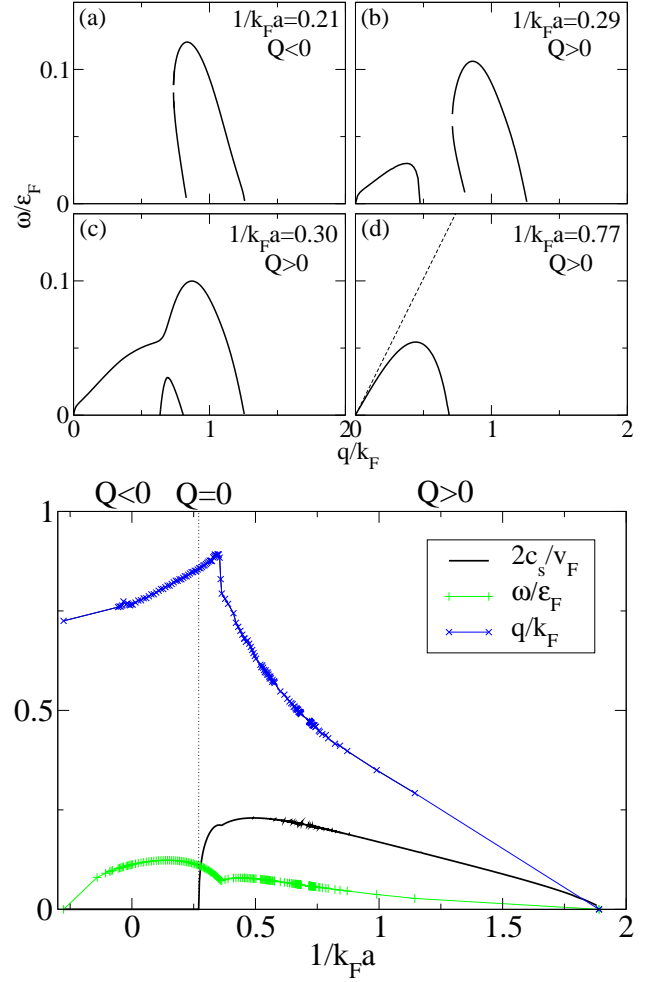


FIG. 3: (Colour online) Upper panels: Unstable modes frequency ω/ε_F ($\omega(\mathbf{q}) \equiv -i\varepsilon(\mathbf{q})$) versus momentum q/q_F for different values of the interaction strength $1/k_F a$ across the spinodal region and for fixed polarisation $m/n = 0.5$. Note that gaps correspond to complex frequencies. Lower panel: Plot of the most unstable mode frequency ω/ε_F (plus green), momentum q/q_F (times blue) and of the sound velocity $2c_s/v_F$ (solid black) across the spinodal region for fixed polarisation $m/n = 0.5$.

where $A = \frac{1}{V} \sum_{\mathbf{k}} \Theta(E_{\mathbf{k}} - h) \frac{\Delta^2}{2E_{\mathbf{k}}^3}$, $B = \frac{1}{V} \sum_{\mathbf{k}} \Theta(E_{\mathbf{k}} - h) \frac{\epsilon_{\mathbf{k}} - \mu}{4E_{\mathbf{k}}^3}$, $R = \frac{1}{V} \sum_{\mathbf{k}} \frac{\Theta(E_{\mathbf{k}} - h)}{8E_{\mathbf{k}}^3}$ and

$$Q = \frac{n}{8m\Delta^2} \left[1 - \frac{h}{2\sqrt{h^2 - \Delta^2}} \frac{\epsilon_+^{3/2} + \epsilon_-^{3/2}}{\epsilon_F^{3/2}} \right]$$

$$P(\varepsilon/q) = \frac{\Delta^2}{2h^2} [\nu_+ L(\varepsilon/v_+ q) + \nu_- L(\varepsilon/v_- q)],$$

with $E_{\mathbf{k}} = \sqrt{(\epsilon_{\mathbf{k}} - \mu)^2 + \Delta^2}$, and where $\nu_{\pm} = \frac{m\epsilon_{\pm}}{\pi^2} v_{\pm}^{-1}$ and $v_{\pm} = dE_{\mathbf{k}}/dk|_{\epsilon_{\pm}}$ are the density of states and velocity at the two solutions ϵ_{\pm} of $E_{\mathbf{k}} = h$ (take $\epsilon_{\pm} = 0 = \nu_{\pm}$ if there is no solution). Note that the phase stiffness $4m\Delta^2 Q$ is the superfluid density¹⁸, which changes sign inside the spinodal region (see Fig. 1).

The higher order terms in the (1, 1) entry of Eq. (14) do not affect the sound velocity c_s , which is the solution of

$$[A + P(c_s)](Q - Rc_s^2) - B^2c_s^2 = 0. \quad (15)$$

For obvious reasons, this analysis closely parallels that of Ref. 27 for Bose-Fermi mixtures, and Eq. 15 reproduces the form of Eq. 6 found earlier.

III. DISCUSSION

At the spinodal lines $A + P(0) = 0$. This is the same condition that was used in Refs. 16,28 to identify the unstable region, although the possibility of metastability was ignored. $A + P(0) < 0$ inside the spinodal region, and one can distinguish two cases: When $Q > 0$ the sound velocity c_s is pure imaginary, while for $Q < 0$ it is in general complex. As a consequence, the unstable mode spectrum changes in character as one moves across $Q = 0$ (see Fig. 3). Approaching the region of negative superfluid density $Q < 0$ from the region $Q > 0$, a second imaginary modes appears (see panel (c) in Fig. 3) and the two merge (panel (b)): The resulting ‘gap’ region corresponds to complex frequencies, implying a ‘flickering’ component to the instability. The most unstable mode always corresponds to a pure imagi-

nary frequency, however. While the most unstable mode frequency and wavevector go to zero on the superfluid side of the spinodal region, the instability towards a Fulde-Ferrell-Larkin-Ovchinnikov (FFLO) phase means that the characteristic wavevector does not go to zero on the normal side¹³. Indeed, one may view the early stages of spinodal decomposition as a transient FFLO state.

The characteristic length and time scales at which inhomogeneities appear as the precursor of phase separation are determined by the most unstable modes. At unitarity $1/k_F a = 0$ and for $T_F = 1\mu\text{K}$, this time scale is of order of $400\mu\text{s}$, which is on the same scale as the condensate formation time, as measured in Ref. 29. The length scale is roughly $1/k_F \simeq 0.1\mu\text{m}$. Both scales become larger as one approaches the spinodal lines, which will always occur somewhere in the trap. The unitarity region may be a suitable place to observe the late stages of spinodal decomposition and the possible existence of a coarsening regime.

In conclusion, we have studied the early stage dynamics of phase separation in polarised Fermi superfluids. We expect that the investigation of these instabilities is within reach of current experiments.

We are grateful to P. Eastham for help with the numerics and to TCM group in Cambridge for the use of computer resources. FMM would like to acknowledge the financial support of EPSRC.

* Electronic address: austen@virginia.edu

† Electronic address: fmm25@cam.ac.uk

¹ C. A. Regal, M. Greiner, and D. S. Jin, Phys. Rev. Lett. **92**, 040403 (2004).

² M. W. Zwierlein, C. A. Stan, C. H. Schunck, S. M. F. Raupach, A. J. Kerman, and W. Ketterle, Phys. Rev. Lett. **92**, 120403 (2004).

³ C. Chin, M. Bartenstein, A. Altmeyer, S. Riedl, S. Jochim, J. H. Denschlag, and R. Grimm, Science **305**, 1128 (2004).

⁴ T. Bourdel, L. Khaykovich, J. Cubizolles, J. Zhang, F. Chevy, M. Teichmann, L. Tarruell, S. J. J. M. F. Kokkelmans, and C. Salomon, Phys. Rev. Lett. **93**, 050401 (2004).

⁵ J. Kinast, S. L. Hemmer, M. E. Gehm, A. Turlapov, and J. E. Thomas, Phys. Rev. Lett. **92**, 150402 (2004).

⁶ M. W. Zwierlein, C. H. Schunck, C. A. Stan, S. M. F. Raupach, and W. Ketterle, Phys. Rev. Lett. **94**, 180401 (2005).

⁷ M. W. Zwierlein, A. Schirotzek, C. H. Schunck, and W. Ketterle, Science **311**, 492 (2006).

⁸ G. B. Partridge, W. Li, R. I. Kamar, Y. Liao, and R. G. Hulet, Science **311**, 503 (2006).

⁹ M. W. Zwierlein, C. H. Schunck, A. Schirotzek, and W. Ketterle, Nature **442**, 54 (2006), cond-mat/0605258.

¹⁰ Y. Shin, M. W. Zwierlein, C. H. Schunck, A. Schirotzek, and W. Ketterle, Phys. Rev. Lett. **97**, 030401 (2006).

¹¹ G. B. Partridge, W. Li, Y. A. Liao, R. G. Hulet, M. Haque, and H. T. C. Stoof, Phys. Rev. Lett. **97**, 190407 (2006).

¹² P. F. Bedaque, H. Caldas, and G. Rupak, Phys. Rev. Lett. **91**, 247002 (2003).

¹³ D. E. Sheehy and L. Radzihovsky, Phys. Rev. Lett. **96**, 060401 (2006).

¹⁴ M. M. Parish, F. M. Marchetti, A. Lamacraft, and B. D. Simons, cond-mat/0605744 (Nat. Phys. to appear).

¹⁵ K. B. Gubbels, M. W. J. Romans, and H. T. C. Stoof, Phys. Rev. Lett. **97**, 210402 (2006).

¹⁶ C.-C. Chien, Q. Chen, Y. He, and K. Levin, Phys. Rev. Lett. **97**, 090402 (2006).

¹⁷ M. Iskin and C. A. R. Sá de Melo, Phys. Rev. Lett. **97**, 100404 (2006).

¹⁸ C.-H. Pao, S.-T. Wu, and S.-K. Yip, Phys. Rev. B **73**, 132506 (2006).

¹⁹ C.-H. Pao, S.-T. Wu, and S.-K. Yip, Phys. Rev. B **74**, 189901(E) (2006).

²⁰ J. D. Gunton, M. S. Miguel, and P. S. Sahni, *Phase Transitions and Critical Phenomena*, vol. 8 (Academic Press, London, 1983).

²¹ J. K. Hoffer and D. N. Sinha, Phys. Rev. A **33**, 1918 (1986).

²² A. J. Bray, Adv. Phys. **51**, 481 (1994).

²³ P. C. Hohenberg and D. R. Nelson, Phys. Rev. B **20**, 2665 (1979).

²⁴ H. B. Callen, *Thermodynamics and an Introduction to Thermostatistics* (John Wiley & Sons, New York, 1985).

²⁵ G. Sarma, J. Phys. Chem. Solids **24**, 1029 (1963).

²⁶ J. R. Engelbrecht, M. Randeria, and C. A. R. Sá de Melo, Phys. Rev. B **55**, 15153 (1997).

²⁷ D. H. Santamore, S. Gaudio, and E. Timmermans, Phys. Rev. Lett. **93**, 250402 (2004).

²⁸ Q. Chen, Y. He, C.-C. Chien, and K. Levin, Phys. Rev. A

74, 063603 (2006).

²⁹ M. W. Zwierlein, C. H. Schunck, C. A. Stan, S. M. F. Raupach, and W. Ketterle, Phys. Rev. Lett. **94**, 180401 (2005).

³⁰ One can in general show that, at the mean-field level, the free energy (1) is a function of m/n only, and conversely the grand canonical potential (3) is function of $h/|\mu|$ only.